2021 IEEE 15th International Conference on Compatibility, Power Electronics and Power Engineering (CPE-POWERENG) | 978-1-7281-8071-7/21/$31.00 ©2021 IEEE | DOI: 10.1109/CPE-POWERENG50821.2021.9501219

Three-phase CLLLC Resonant Converters

Juan Ignacio Núñez
Power Electronics Systems Group
Carlos III University of Madrid
Madrid, Spain

Andrés Barrado
Power Electronics Systems Group
Carlos III University of Madrid
Madrid, Spain
andres.barrado@uc3m.es

Antonio Lázaro
Power Electronics Systems Group
Carlos III University of Madrid
Madrid, Spain
alazaro@ing.uc3m.es

Pablo Zumel
Power Electronics Systems Group
Carlos III University of Madrid
Madrid, Spain
pzumel@ing.uc3m.es

***Abstract*—A three-phase resonant converter allows high-density operations than a one-phase resonant converter. These one-phase converters, such as LLC and CLLLC, have already been investigated and optimized by many authors. These papers study the different topologies and connections that a three-phase CLLLC resonant converter can present. Two main topologies are considered in this paper. They both exhibit a three-phase bridge as input and a three-phase transformer that integrates each phase's resonant tank. The difference between both topologies emerges from the output rectifier. One topology uses a three-phase bridge as a rectifier, whereas the other uses three one-phase full-bridge. The three-phase bridge rectifier and a delta connection on both sides of the transformer allow a faster response while reducing the RMS current through the transformer. In addition, a better PCB integration can be acquired.**

***Keywords*—Resonant converter, CLLLC, delta, star, ZVS, integrated magnetics, three-phase.**

I. Introduction

Resonant converters are frequently used in applications such as battery charging, smart grids, and renewable energy technologies. This high demand is due to the multiple benefits resonant converters have, for instance, high efficiency, galvanic isolation, or bidirectional energy flow. Another advantage of these converters is that transistors from the primary side of the converter can operate with Zero Voltage Switching (ZVS) in a wide power range.

Two of the most studied single-phase resonant converters are the LLC and the CLLLC [1]–[4]. The design of both converters has been studied for years, obtaining efficient and reduced size models by integrating magnetics 9 This concept consists of building a magnetic core that integrates the resonant inductor as leakage inductance. When designing the resonant tank, choosing a high resonant frequency reduces the size of the passive components, allowing combining the passive elements into a single core [3]. Three-phase resonant converters can use this concept, integrating three single-phase cores into one core. In [7], a study based on Lagrangian dynamics shows how a three-phase magnetic core can be as efficient as three single-phase ones. More literature is found when looking for three-phase LLC integrated magnetics. In [7]–[11], the resonant inductors are integrated into the magnetics of a three-phase core. In [9], an overview of many studies is made, presenting a way of integrating magnetics into an EE core, which can be applied in industrial applications.

Furthermore, a three-phase CLLLC converter was studied in [10] for a 12.5 kW output power application. In this paper, a planar transformer is designed by integrating the windings in a PCB. Planar transformers in resonant converters have become a new trend that paves the way to design a fully integrated converter. A technique to develop the windings of a planar transformer into PCB layers can be reviewed in [11]. The main drawbacks faced by high-frequency converters are EMI noise and switching losses. Both are related to increasing the frequency. This fact limits the design to a certain extent. Likewise, when implementing the passive components of three-phase converters in the resonant tank, they have a tolerance. This difference in the values, be it even little, can result in a current imbalance [9]. Imbalances can be reduced by selecting the connection of the resonant capacitors between phases, as explained in [10].

This paper provides a study about the different connections that both topologies can present, highlighting each topology's benefits and limitations. The conclusions are made by considering the voltage and the current stress existent in the components of the resonant tank and the open-loop response of each converter topology for each connection model. A total of twenty models are simulated in this work.

II. Topology Description & Design Methodology

The three-phase CLLLC resonant converter models studied in this paper contain a three-phase bridge as input and a rectifier bridge as output, which differs between a three-phase rectifier bridge and three single-phase full-bridge topologies. The resonant tank consists of a resonant inductance per phase. This tank has on each side a resonant inductor integrated into a three-phase transformer and a resonant capacitor. A scheme of this converter is shown in Fig. 1.

The design of the converter starts with the selection of the value of the resonant tank's passive components. A method to approach an optimized design of a CLLLC resonant tank is explained in [2]. Most of the optimized designs are made by the *First Harmonic Approximation (FHA)* approach.This technique simplifies the system into the linear circuit shown in Fig. 2.

This Work has been partially supported by the Spanish Ministry of Science, Innovation, and Universities through the research project HIDRON (PID2020-116500RB-I00) and the project Challenges Collaboration ELECTRA (RTC-2017-6667-4), and by the Regional Council of Science, Universities and Innovation of the Community of Madrid through the research project DROMADER-CM (Y2020/NMT-6584).

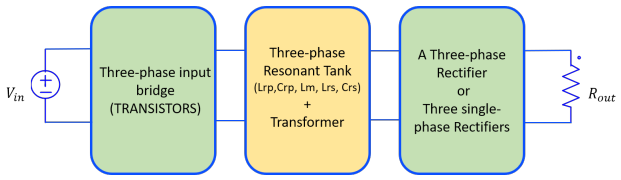

Fig. 1. Schematic of a three-phase CLLLC resonant converter.

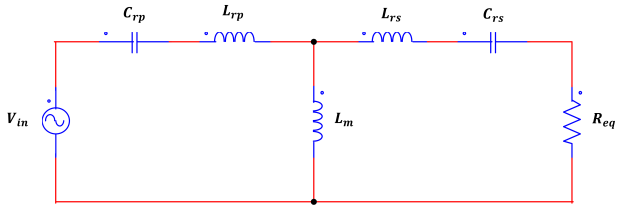

Fig. 2. Lineal circuit of a CLLLC Resonant Tank by FHA approach.

$$H(s) = \frac{\left(k \cdot f_n^2\right)}{\sqrt{\left((k+1) \cdot f_n^2 - 1\right)^2 + \left(k \cdot Q \cdot \left(\left(f_n^2 - 1\right) \cdot f_n\right)^2\right)}} \quad (1)$$

$$f_n = \frac{f_{sw}}{f_r} \quad (2)$$

$$Q = \frac{z_r}{R_{eq}} \quad (3)$$

$$Z_r = \sqrt{\frac{L_r}{C_r}} \quad (4)$$

$$L_{rp} = L_r \quad (5)$$

$$C_{rp} = C_r \quad (6)$$

$$K = \frac{Lm}{Lr} \quad (7)$$

$$n = \frac{N_p}{N_s} \quad (8)$$

$$f_r = \frac{1}{2\pi\sqrt{L_r C_r}} \quad (9)$$

$$L_{rs} = \frac{L_r}{n^2} \quad (10)$$

$$C_{rs} = n^2 C_r \quad (11)$$

The equations above are used in the design process, where fn is the normalized working frequency obtained by dividing the working frequency by the chosen resonant frequency. Furthermore, K is defined by the ratio between the magnetic inductance and the resonant inductance, Q is the quality factor, n is the transformer's turns ratio defined as primary over secondary, and Zr is the characteristic impedance. Lrp, Lrs, Crp, and Crs values correspond to the inductance and capacitance values of the resonant tank reflected on the primary side, being Lr and Cr the equivalent resonant value with an n ratio equal to the unit. Moreover, the transfer function (1) is obtained from the linear circuit by substituting the parameters for f_n, Q and K, making use of the equations (2,3,7) as illustrated in [4]. By modifying the values of Q and establishing a value for K, Fig. 3 is obtained. Each curve represents the system's gain (y-axis) as a function of the normalized operating frequency (x-axis). The value of Q is selected by choosing the curve that meets the gain requirements at the chosen operating frequency. The chosen operating frequency is usually over the resonant frequency due to the ZVS working principle in the primary transistors.

The last step of the design is establishing the relation between the output resistance and the equivalent resistance, re-

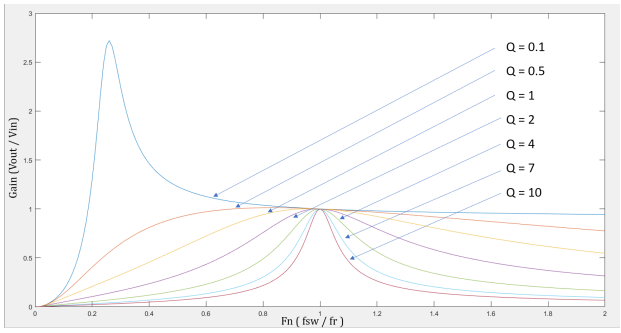

Fig. 3. Lineal circuit of a CLLLC Resonant Tank by FHA approach.

ferred to the primary side of the linear circuit. The value of the equivalent resistance depends on the type of rectifier bridge, half-bridge or full-bridge rectifier. The relation between the equivalent resistance (Req) and the output resistance (Ro) is obtained by making the AC power consumed by Req equal to the DC power consumed by Ro. The three-phase rectifier presents three half-bridges resulting in an equivalent resistance equal to (12). In contrast, the three single-phase full-bridge relation is shown in (13). Once the relation is set, the design process introduces the input parameters in the equations (4-6, 9-11) to obtain the numerical parameter value of the resonant tank components of each phase.

$$R_{eq} = \frac{6}{\pi^2} \cdot n^2 \cdot R_o \quad (12)$$

$$R_{eq} = \frac{8}{\pi^2} \cdot n^2 \cdot R_o \quad (13)$$

A. *Three-phase output rectifier*

The first topology uses a three-phase bridge as input, three CLLLC resonant tanks, and a three-phase transformer. The output block of this converter is composed of a three-phase bridge. This output bridge rectifies the current that comes out of each leg of the transformer. A three-phase CLLLC resonant converter with FYYL connection and three-phase output rectifier topology is shown in Fig. 4. The connection nomenclature is explained in the next section. The symmetry between the input and output bridges confers a unity voltage gain on this topology, working at the resonant frequency.

B. *Three one-phase full-bridge rectifier*

The second topology studied has the same three-phase input bridge, a three-phase transformer, and three CLLLC resonant tanks as the first topology. Besides, the second topology uses three single-phase full-bridge to rectify the current. A three-phase CLLLC resonant converter with FYPL connection and three one-phase full-bridge topology is illustrated in Fig. 5. The asymmetry between the input and output bridges modifies the gain relation compared to the symmetric model. In this case, the relation is one-half when working at the resonant frequency. This topology is studied and developed in [10].

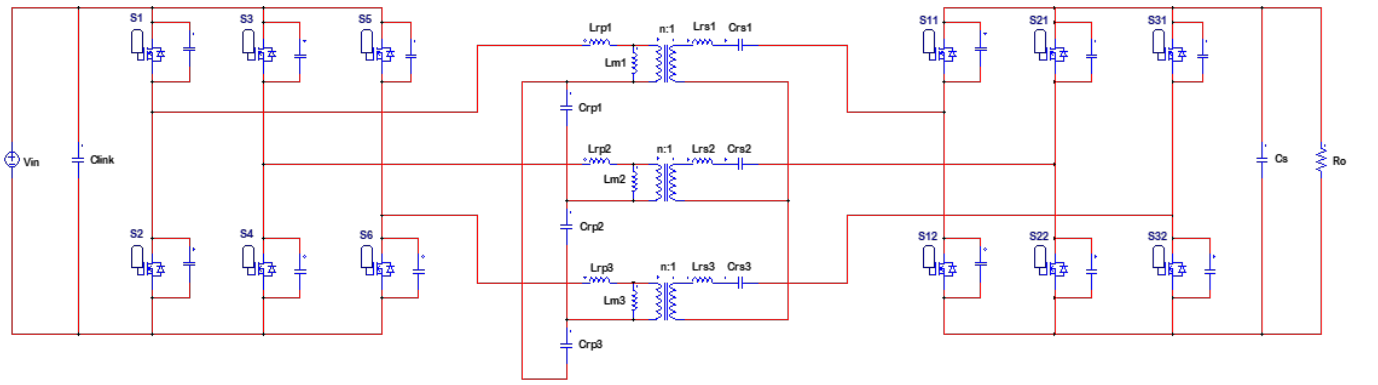

Fig. 4. Three-phase CLLLC resonant converter with FYYL connection and a three-phase output rectifier.

III. Connections of the Resonant Tank

A three-phase resonant converter offers a wide range of possibilities when selecting the connections for the resonant tank of each phase. The capacitors can be connected in delta or star. The two types of connection supply the capacitors with self-balancing of the current in each phase, as explained in [10]. The star connection can produce difficulties in the start-up due to direct current bias; this issue can be solved with the delta connection [10]. The main difference between both connection types is due to the current that runs through them. A capacitor's delta connection provides a phase current and line voltage stress, whereas a star connection produces line current and phase voltage stress. In addition, the value obtained in (6) is three times the value of the capacitor when working with a delta connection. If a star connection is applied, the value corresponds to the one obtained in the previous design methodology. From now on, the connection of the capacitors is named by the letter F (phase current) when applying delta connection and by the letter L (line current) with star connection.

As seen with the resonant tank capacitors on both sides of the converter, the three-phase transformer windings can also be connected in delta or star. Similarly, the delta connection reduces the current through each winding, including the magnetizing current, but applies line voltage to each winding. The contrary happens with the star connections of the windings. As well as with the capacitors, a change from the design's result happens when applying a windings delta connection. In this case, the delta connection multiplies the resonant inductance obtained in (5) by three. As the parameter k relates to magnetizing inductance and resonant inductance, the magnetizing inductance is also increased by a factor of three.

Next, to denote the connection type of the transformer windings in each model, the delta connection is named with the letter D, and the star connection is named with the letter Y. The topology with three single-phase full-bridge as rectifier has a determined output connection, making capacitors connected in

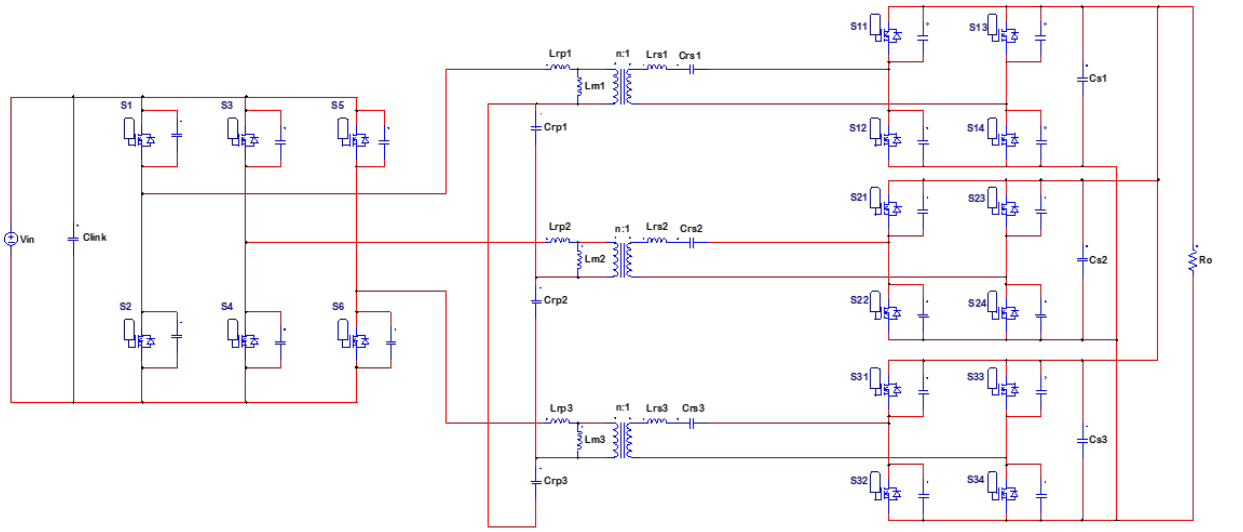

Fig. 5. Three-phase CLLLC resonant converter with FYPL connection and three one-phase full-bridge rectifier.

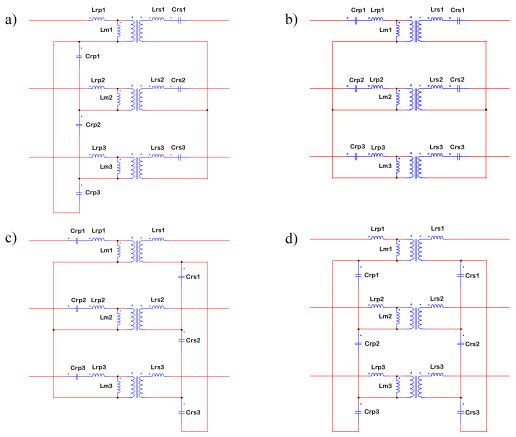

Fig. 6. Connection YY between the windings of the transformer. a) FYYL b) LYYL c) LYYF d) FYYF

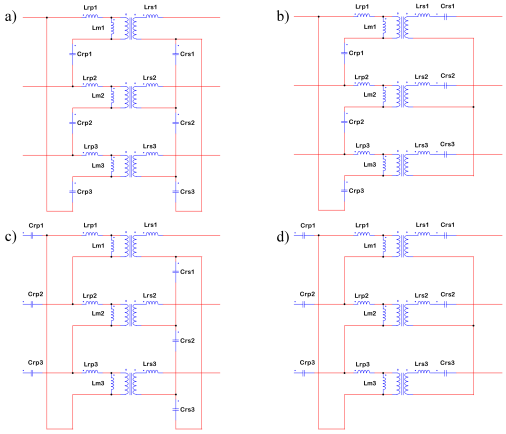

Fig. 8. Connection DY between the windings of the transformer. a) FDYF b) FDYL c) LDYF d) LDYL

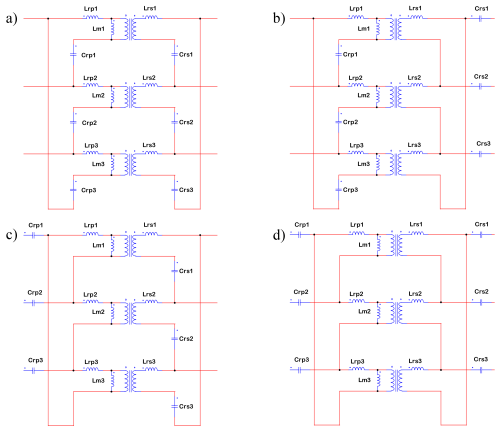

Fig. 7. Connection DD between the windings of the transformer. a) FDDF b) FDDL c) LDDF d) LDDL

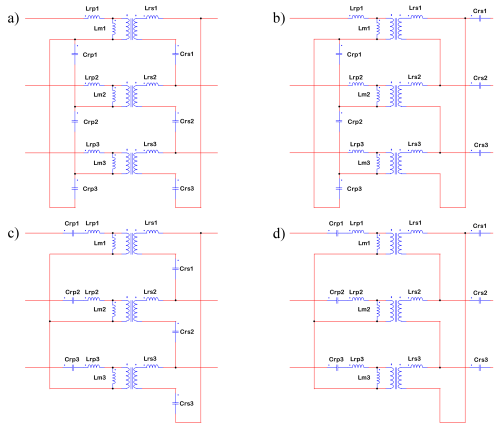

Fig. 9. Connection YD between the windings of the transformer. a) FYDF b) FYDL c) LYDF d) LYDL

L. With the objective to differentiate this connection from the others, it is named by the letter P. Combining the assessed nomenclature, connections in Fig. 6, 7, 8, and 9 are shown. A total of twenty connection models are obtained.

The models in Fig. 6 have a YY connection of the transformer windings. A model with this connection was studied in [10]. In contrast, a YD connection model was studied for a three-phase LLC converter in [11]. The YY and DD connections are symmetric with respect to the primary and secondary sides of the transformer. These connection models have a unity gain relation. In contrast, when applying a DY or a YD connection model, the gain relation of the transformer increases or decreases by a factor of the square root of three, respectively. The adjustment can be easily obtained by changing the relation of the transformer (n). The weakness of the modification is noticed when observing the stress applied to the components, as it produces an unbalance in the voltage stress between the primary and secondary sides. This unbalance increases the amount of voltage stress on one of the converter's sides, where bigger passive components are needed hindering the integration.

IV. Parameters of the Designed Converter

Once the topology description and a review of the design methodology are made, the converter's input parameters are listed. The design has a 400 V input voltage from the Power Factor Correction stage (PFC), a 360 V output voltage, and a 2 kW maximum output power. The scheme of the battery charger is shown in Fig. 10. The 500 kHz resonant frequency is chosen to be similar as in [10] to pursue integrated magnetics small passive elements for a suitable transformer design.

The parameter K selected for the design is 15. This value is obtained from [12], where a study about which value of K provides the lowest losses is done.

The design values mentioned up to now keep constant for the design of the twenty models. An adjustment in the transformer relation n and in the dead time is made to obtain the same input and output voltages at 2 kW, operating at the same frequency. The calculated parameters for the simulations are listed in Table 1.

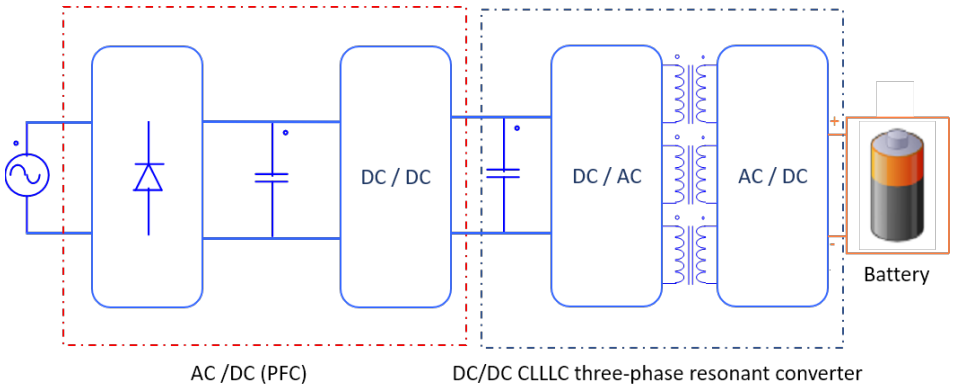

Fig. 10. Schematic of the application, including a three-phase CLLLC Resonant Converter and a PFC.

Table 1. Designs of the three-phase CLLLC Resonant Converter.

Models	*Vin (V)*	*Pout (kW)*	*Fres (kHz)*	*Rout (Ω)*	*Lrp (μH)*	*Lrs (μH)*	*Crp (nF)*	*Crs (nF)*	*Lm (μH)*	*K*	*n*
FYYF	400	2	500	61.25	6.51	6.51	5.2	5.2	97	15	1
FYYL	400	2	500	61.25	6.51	6.51	5.2	15.54	97	15	1
LYYF	400	2	500	61.25	6.51	6.51	15.5	5.2	97	15	1
LYYL	400	2	500	61.25	6.51	6.51	15.5	15.54	97	15	1
FTTF	400	2	500	61.25	19.5	19.5	5.2	5.2	291	15	1
FTTL	400	2	500	61.25	19.5	19.5	5.2	15.54	291	15	1
LTTF	400	2	500	61.25	19.5	19.5	15.5	5.2	291	15	1
LTTL	400	2	500	61.25	19.5	19.5	15.5	15.54	291	15	1
FTYF	400	2	500	61.25	58.5	2.2	1.73	15.54	873	15	1.73
FTYL	400	2	500	61.25	58.5	2.2	1.73	46.52	873	15	1.73
LTYF	400	2	500	61.25	58.5	2.2	5.2	15.54	873	15	1.73
LTYL	400	2	500	61.25	58.5	2.2	5.2	46.52	873	15	1.73
FYTF	400	2	500	61.25	2.2	58.5	15.46	1.75	32.3	15	0.58
FYTL	400	2	500	61.25	2.2	58.5	15.46	5.22	32.3	15	0.58
LYTF	400	2	500	61.25	2.2	58.5	46.2	1.75	32.3	15	0.58
LYTL	400	2	500	61.25	2.2	58.5	46.2	5.22	32.3	15	0.58
LYPL	400	2	500	61.25	1.62	26	62.1	3.9	48.5	15	0.5
FYPL	400	2	500	61.25	1.62	26	20.8	3.9	48.5	15	0.5
FTPL	400	2	500	61.25	16.9	7.52	6.95	11.63	252	15	0.865
LTPL	400	2	500	61.25	16.9	7.52	20.8	11.63	252	15	0.865

A Three-phase rectifier Three single-phase rectifier Resonant tank component value

V. Simulations of the Designs

In this section, a simulation of all the models is made using the software PSIM. To obtain an output voltage of 360 V in open loop, an operating frequency of 550 kHz is used for all the models. The dead time of each model is varied to obtain the same output voltage and to ensure ZVS in the transistors of the primary side. This operation is shown in Fig. 11. In Fig. 12, the waveforms of the passive components in the resonant tank are shown. The current waveforms of each phase are balanced. It happens because the passive components of each phase have an equal value in the simulations. When implementing the converter, each passive component has a tolerance, resulting in the current unbalanced distribution in each phase. A three-phase transformer is used to obtain flux cancelation between phases leveling the currents.

In the simulations of this section, three single-phase transformers are used, providing the peak stress value in all the passive components. The simulation of the twenty models is carried out, and the peak stress values of the converter components are measured. The voltage in the primary side

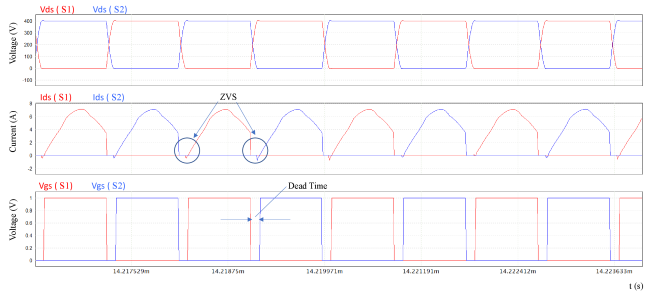

Fig. 11. Primary transistors currents and voltages of the three-phase CLLLC Resonant Converter with FYYL connection working under ZVS condition.

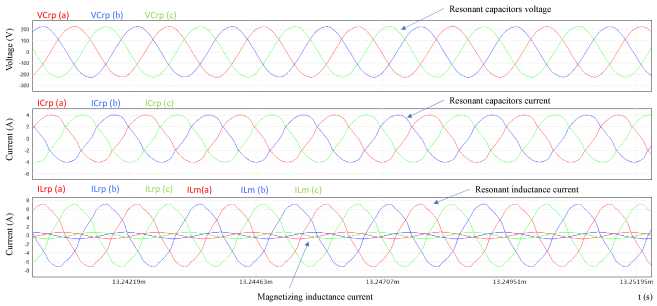

Fig. 12. Waveforms of the passive components inside the resonant tank of the three-phase CLLLC Resonant Converter with FYYL connection.

transistors is 400V, while on the secondary side, the output voltage remains 360 V for all models. The current is 6.8 A in the primary side transistors and 6.4 A in the secondary side transistors for the three-phase bridge model. However, the current in the three full-bridge model is 3.2 A. This maximum voltage on the transistors is presented in Fig. 13 and the maximum current stress across the transistors is presented in Fig.14.

On the one hand, the three-phase output bridge needs half of the switches required in the three full-bridge rectifiers. On the other hand, doubling the number of transistors results in reducing the current by half.

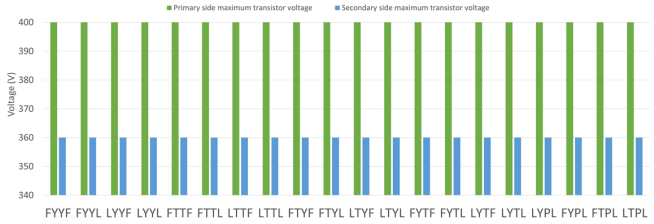

Fig. 13. Voltage in the transistors of the input and output bridges of all the models.

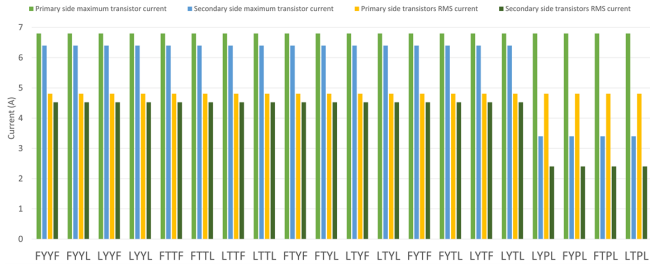

Fig. 14. Current in the transistors of the input and output bridges of all the models.

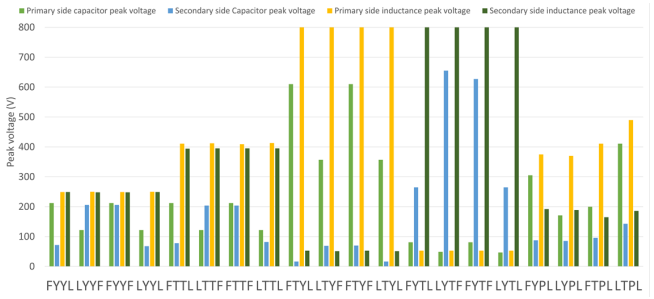

Fig. 15. Peak voltage in the passive components of the resonant tank of all models.

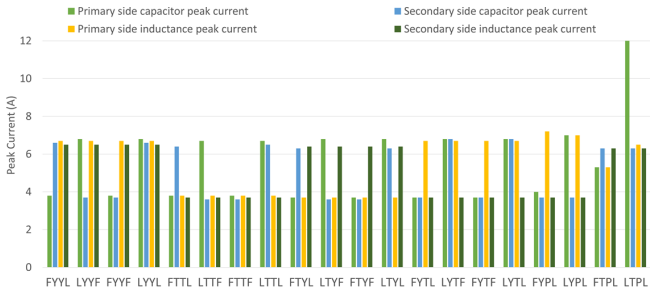

Fig. 16. Peak current across the passive components of the resonant tank of all models.

In Fig. 15 and Fig. 16 can be noticed that the connection of the resonant tank varies the voltage and current stress values in the passive components. In Fig. 15, the peak value of the voltage for each connection model is displayed, while Fig. 16 shows the current peak through the components in each model. The three-phase models with YY connection are the standard models used in a three-phase LLC or three-phase CLLLC resonant converter. This connection is used as a reference to compare with the rest of the models. The models with DD connection have less current through the tank, as the impedance is higher, but the voltage increases due to the same factor. Models with a DY or a YD connection provide a variation in the stress due to the connection type and a change in the stress caused by modifying the ratio of the transformer n.

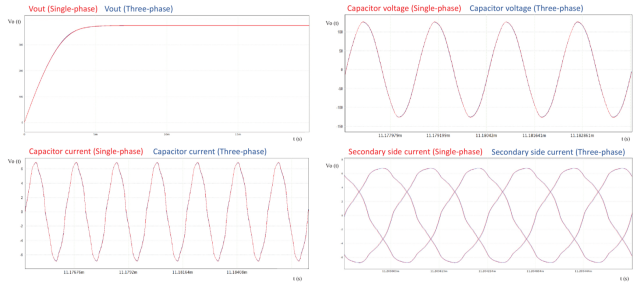

Fig. 17. Waveforms in a three-phase CLLLC resonant converter with LDDL topology, using three one-phase transformers and one three-phase transformer under identical conditions and passive component values.

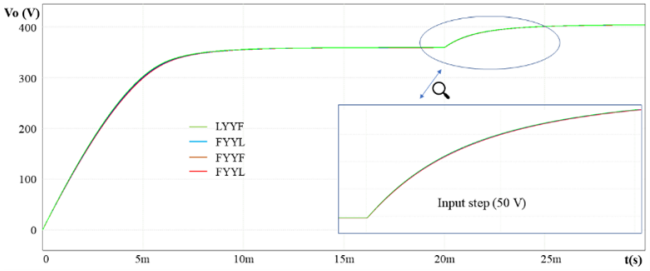

Fig. 18. Start-up and input voltage step of 50 V in all YY connection models with a three-phase output rectifier.

A comparison between three one-phase transformers against one three-phase transformer is illustrated in Fig. 17. This verification is made by introducing the same passive component value between phases. The main difference between both models is contributed by the three-phase transformer, where flux cancelation between phases can be obtained [10]. For our simulations, three single-phase transformers can be used.

An open-loop simulation of the models is carried out to study each connection's input voltage step response. To study the open-loop dynamic response of all the models, the start-up process is not considered. The start-up process of the resonant converters is modulated by applying a soft start. This process avoids very high currents through the components, reducing the conduction loss and keeping away from overheated components.

The first concept acquired from the simulations is that the response to an input step does not change by varying the capacitors into line or phase current, as shown in Fig. 18, where the dynamic behavior of all the possible connections for a YY model is depicted. The following premise obtained by the simulations is illustrated in Fig. 19, where the responses are pointed up. The faster ones are the YY and DD models by comparison with the DY and YD models.

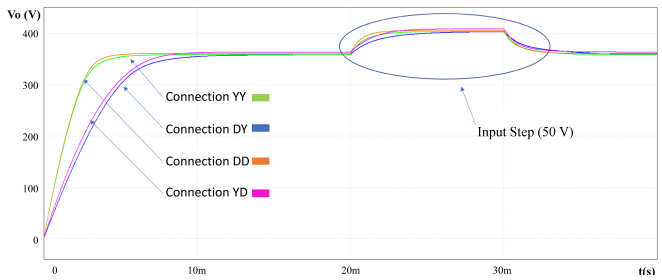

Fig. 19. Start-up and input voltage step of 50 V during 10 milliseconds in the YY, DD, DY, and YD connection models with a three-phase output rectifier.

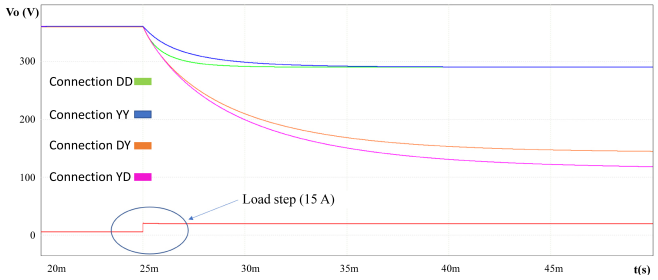

Fig. 20. Load current step of 15 A in YY, DD, DY, and YD models with a three-phase output rectifier.

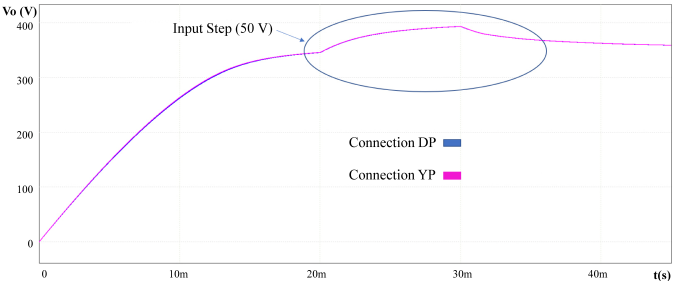

Fig. 21. Start-up and input voltage step of 50 V during 10 milliseconds in all the DP and YP models for three full-bridge output rectifiers.

A load step response is presented in Fig. 20 for the YY, DD, DY, and YD connections with a three-phase output rectifier. The DD connection is faster than the YY connection, having the same output voltage decrease for both connections. The connections with the biggest voltage decrease are DY and YD. A simulation of the three full-bridge topology connections is shown in Fig. 21, obtaining almost the same response for all the models.

Therefore, the response varies between the chosen topologies. A three-phase rectifier as output gives faster response than three single-phase rectifiers. The models with three-phase output rectifier and YY or DD connection give the best results under a load step. Both models are also the most suitable for a bidirectional operation when looking for a component stress reduction and symmetry. In particular, the delta connection reduces the intensity through the transformer windings, which can be taken in advance for PCB integration. Changing the capacitor connection does not provide a different response. Bearing in mind the aforementioned statements, the FDDF connection with a three-phase output bridge is the most suitable for a fully integrated implementation.

VI. Conclusion

Twenty different connection models combining two topologies are studied for a three-phase CLLLC resonant converter. Firstly, a guided design has been shown with the particularities of each topology. Next, all the connections have been presented by combining the connection of the capacitors between phase current (F) or line current (L) along with the interwinding connection between delta (D), star (Y), and parallel (P) for the models with three full-bridge rectifiers. Thirdly, a three-phase CLLLC resonant converter design has been done for a bidirectional battery charger with 400 V as input voltage and 360 V as output voltage, working at 550 kHz.

The values for the different connection models of each topology have been listed in . These values are obtained with the design methodology from the previous sections. The last step is to simulate with PSIM the twenty models to obtain the peak value of both voltage and current in all the converter components. The stress in the components has evidenced two premises to bear in mind when designing the converter. The connection model of the resonant tank and the transformer does not affect the input and output bridges.

The second highlight comes from the interwinding connection. The star and delta connection election modifies the voltage and the current peak, increasing or decreasing the RMS value. For an integrated converter model with PCB windings, where the resonant frequency is high, reducing the RMS current through the windings is essential to achieve high power density through the transformer windings.

The selection of the capacitor connection between line or phase current can be made using the study [10] as a reference. As explained in Section III, the phase current connection produces a better current balancing between phases when a tolerance appears in the passive elements.

In addition to the previous simulations, a study of the response is made for all the connection models. These simulations show how the models' response with three-phase bridge topology is faster than the converters with three full-bridge rectifiers.

This means that the three-phase output topology enables a much faster converter control, allowing higher frequency designs. In contrast, a benefit of using a rectifier based on three full-bridge is implementing this converter in applications with different loads. Another advantage of selecting this second topology is that the transistors in a three-phase bridge conduct the double current than the full-bridge connection, a concept that can be taken in advance to reduce conduction losses.

The chosen topology is the three-phase bridge in input and output, with the capacitors receiving phase current and a DD connection between windings. The resultant model has an FDDF connection, as shown in Fig. 22. This model confers

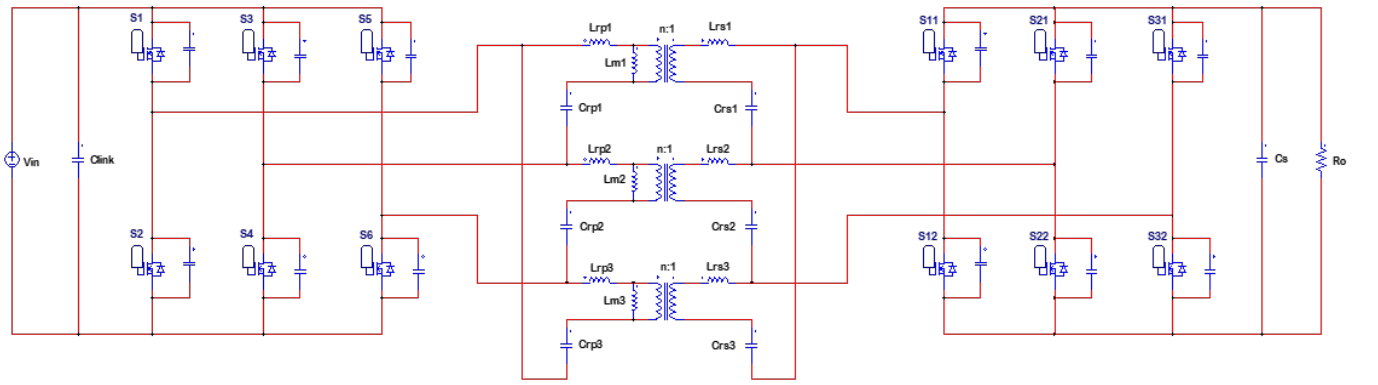

Fig. 22. Three-phase CLLLC resonant converter with FDDF connection and three-phase output rectifier.

lower current through the transformer, where a better converter integration can be acquired.

The future work consists of integrating the model in a PCB, making use of planar magnetics. Another concept to study is common mode noise reduction methods applied to this model based on introducing shielding layers between the windings of the transformer.

REFERENCES

[1] G. Liu, D. Li, J. Q. Zhang, B. Hu and M. L. Jia, "Bidirectional CLLC resonant DC-DC converter with integrated magnetic for OBCM application," 2015 IEEE International Conference on Industrial Technology (ICIT), Seville, Spain, 2015, pp. 946-951, doi: 10.1109/ICIT.2015.7125219.

[2] J. Jung, H. Kim, M. Ryu and J. Baek, "Design Methodology of Bidirectional CLLC Resonant Converter for High-Frequency Isolation of DC Distribution Systems," in IEEE Transactions on Power Electronics, vol. 28, no. 4, pp. 1741-1755, April 2013, doi: 10.1109/TPEL.2012.2213346.

[3] Wenduo Liu and J. D. van Wyk, "Design of integrated LLCT module for LLC resonant converter," Twentieth Annual IEEE Applied Power Electronics Conference and Exposition, 2005. APEC 2005., Austin, TX, USA, 2005, pp. 362-368 Vol. 1, doi: 10.1109/APEC.2005.1452954.

[4] H. Wen, D. Jiao and J. Lai, "Optimal Design Methodology for High Frequency GaN Based Step-up LLC Resonant Converter," 2019 IEEE 4th International Future Energy Electronics Conference (IFEEC), Singapore, 2019, pp. 1-5, doi: 10.1109/IFEEC47410.2019.9014657.

[5] M. Li, Z. Ouyang, B. Zhao and M. A. E. Andersen, "Analysis and modeling of integrated magnetics for LLC resonant converters," IECON 2017 - 43rd Annual Conference of the IEEE Industrial Electronics Society, Beijing, China, 2017, pp. 834-839, doi: 10.1109/IECON.2017.8216144.

[6] B. Li, Q. Li, F. C. Lee and Y. Yang, "A symmetrical resonant converter and PCB transformer structure for common mode noise reduction," 2017 IEEE Energy Conversion Congress and Exposition (ECCE), Cincinnati, OH, USA, 2017, pp. 5362-5368, doi: 10.1109/ECCE.2017.8096898.

[7] M. Noah, K. Umetani, S. Endo, H. Ishibashi, J. Imaoka and M. Yamamoto, "A Lagrangian dynamics model of integrated transformer incorporated in a multi-phase LLC resonant converter," 2017 IEEE Energy Conversion Congress and Exposition (ECCE), Cincinnati, OH, USA, 2017, pp. 3781-3787, doi: 10.1109/ECCE.2017.8096668.

[8] M. Noah, S. Kimura, S. Endo, M. Yamamoto, J. Imaoka, K. Umetani, W. Martinez "A Novel Three-phase LLC Resonant Converter with Integrated Magnetics for Lower Turn-off losses and Higher Power Density," Conf. Proc.- IEEE Appl. Power Electron. Conf. Expo. (APEC), pp. 1–8, March, 2017.

[9] M. Noah et al., "Magnetic Design and Experimental Evaluation of a Commercially Available Single Integrated Transformer in Three-Phase LLC Resonant Converter," in IEEE Transactions on Industry Applications, vol. 54, no. 6, pp. 6190-6204, Nov.-Dec. 2018, doi: 10.1109/TIA.2018.2856631.

[10] B. Li, Q. Li and F. C. Lee, "A WBG based three phase 12.5 kW 500 kHz CLLC resonant converter with integrated PCB winding transformer," 2018 IEEE Applied Power Electronics Conference and Exposition (APEC), San Antonio, TX, USA, 2018, pp. 469-475, doi: 10.1109/APEC.2018.8341053.

[11] M. Noah et al., "A novel three-phase LLC resonant converter with integrated magnetics for lower turn-off losses and higher power density," 2017 IEEE Applied Power Electronics Conference and Exposition (APEC), Tampa, FL, USA, 2017, pp. 322-329, doi: 10.1109/APEC.2017.7930712.

[12] B. Li, Q. Li and F. C. Lee, "A novel PCB winding transformer with controllable leakage integration for a 6.6kW 500kHz high efficiency high density bi-directional on-board charger," 2017 IEEE Applied Power Electronics Conference and Exposition (APEC), Tampa, FL, USA, 2017, pp. 2917-2924, doi: 10.1109/APEC.2017.7931111.